buildings

MDPI

Article

Mechanical Properties, Workability, and Experiments of Reinforced Composite Beams with Alternative Binder and Aggregate

Zuzana Marcalikova [1], Jan Jerabek [1,*], Radoslav Gandel [1], Roman Gabor [2], Vlastimil Bilek [1] and Oldrich Sucharda [1]

[1] Department of Building Materials and Diagnostics of Structures, Faculty of Civil Engineering, VSB—Technical University of Ostrava, Ludvíka Podéště 1875/17, 70800 Ostrava-Poruba, Czech Republic; zuzana.marcalikova@vsb.cz (Z.M.); radoslav.gandel@vsb.cz (R.G.); vlastimil.bilek@vsb.cz (V.B.); oldrich.sucharda@vsb.cz (O.S.)

[2] Centre for Energy and Environmental Technologies, VSB—Technical University of Ostrava, 17. Listopadu 15, 70800 Ostrava-Poruba, Czech Republic; roman.gabor@vsb.cz

* Correspondence: jan.jerabek@vsb.cz

Abstract: Arguably the most important element in the sustainability of concrete development is the discovery of an optimal sustainable binder and substitution for the increasingly depleted reserves of natural aggregates. Considerable interest has been shown in alkali-activated materials, which possess good characteristics and could be considered environmentally friendly because of their use of secondary materials in production. The aim of this study was the determination of the mechanical properties of three different mixtures based on the same locally accessible raw materials. The reference mixture contained Portland cement, the second mix contained a finely ground granulated blast furnace slag instead of cement, and the third mixture contained a portion of light artificial aggregate. The experiments focused on the testing and mutual comparison of the processability of the fresh mixture and mechanical characteristics (like compressive and flexural strength, as well as resistance to high temperatures and surface layer tear strength tests). Reinforced concrete beams without shear reinforcement and with three levels of reinforcement were also tested with a three-point bend test. The results show that, overall, the mechanical properties of all the tested mixtures were similar, but each had its own disadvantages. For example, the blast furnace slag-based mixture had a more vulnerable surface layer or a debatable loss of bulk density in the light aggregate mix at the expense of the mechanical properties. One of the main results of the research is that it was possible to technologically produce beams from the alkali-activated concrete (AAC) mixture. Then, the performed beam experiments verified the mechanism of damage, collapse, and load capacity. The obtained results are essential because they present the use of AAC not only in laboratory conditions but also for building elements. In beams without shear reinforcement, the typical tensile cracks caused by bending and shear cracks appeared under loading, where their character was affected depending on the degree of beam reinforcement and loading.

Keywords: concrete; cementless concrete; reinforced concrete beam without shear reinforcement; mechanical properties; mixture

check for updates

Citation: Marcalikova, Z.; Jerabek, J.; Gandel, R.; Gabor, R.; Bilek, V.; Sucharda, O. Mechanical Properties, Workability, and Experiments of Reinforced Composite Beams with Alternative Binder and Aggregate. *Buildings* **2024**, *14*, 2142. https://doi.org/10.3390/buildings14072142

Academic Editors: Kamila Kotrasová, Dušan Katunský, Martina Zeleňáková and Peter Mésároš

Received: 14 May 2024
Revised: 26 June 2024
Accepted: 2 July 2024
Published: 12 July 2024

Copyright: © 2024 by the authors. Licensee MDPI, Basel, Switzerland. This article is an open access article distributed under the terms and conditions of the Creative Commons Attribution (CC BY) license (https://creativecommons.org/licenses/by/4.0/).

1. Introduction

Concrete is generally understood as a material with very advantageous properties, such as high compressive strength, resistance to negative environmental influences, impermeability to water, and the workability of the fresh mixture. However, it also has several disadvantages, such as high weight and density, low strength in split tensile tests, low flexural and shear strengths, high thermal and sound conductivity, and higher demands for production, especially from an ecological point of view [1]. As a building material,

concrete is perhaps the most widely used of all, and, usually, depending on its application in a structure, specific versions of it are used, such as high-performance concrete [2,3], fiber-reinforced concrete [4], etc. Concrete is based on Portland cement as a binder, to which the issue addressed in this paper is related. The production of cement is a very energy-intensive process, whereby limestone is heated to a sintering temperature of 1450 °C in cement rotary kilns. During the thermal decomposition of limestone ($CaCO_3$), the necessary CaO is produced for the subsequent production steps, but a large amount of greenhouse gas CO_2 is also released (contributing up to 9% of the global CO_2 production) [5]. Thus, the current efforts to be friendlier to the environment and natural resources have driven innovations in concrete production [6]. Much attention is paid to the by-products of industrial production, specifically blast furnace slag and power plant fly-ash [7]. Currently, there are several options for applying the above-mentioned by-products in combination with suitable additives and admixtures, whereby Portland cement can be replaced partially (hybrid cements [7–9]) or completely [10], while maintaining good mechanical properties and durability [10–14]. However, during research into the application of these more environmentally friendly binders, problems have also been encountered, such as high shrinkage, rapid setting, short processing time, or the complex and not yet fully understood chemistry [13,14].

When researching materials' properties, their structural use cannot be neglected. In this case, beams without shear reinforcement were chosen as the structural element to be examined; from a structural and technological point of view, this is an effective solution that utilizes reinforcements and concrete. For concrete, it is important that, upon closer study of the typical shear failure mechanism, a multiaxial state of tension be created; i.e., the mechanical properties in terms of the compressive and split tensile strengths are important [15]. In general, however, it is possible to distinguish several possibilities of beam collapse. In the case of a theoretical description of the mechanism, it is advisable to use generalized numerical models and higher mathematics that relate to individual types of beam collapse. However, the typical approach within the design standards represents a rather significant simplification of the theoretical solution as it is based only on the compressive strength in the case of concrete. Regarding the mentioned theoretical and practical circumstances, it is necessary to pay attention to this issue. There are several recommendations and research projects that address the mechanical properties and shear failure of concrete, which include those in [15–22]. However, the existing knowledge cannot be easily transferred, for example, from non-typical concretes and concrete mixtures as the research in the field of material engineering and concrete mixture design is not so extensive.

Resistance to high temperatures—more precisely, 600 °C and 900 °C—was also included in the experimental program. The temperature of 600 °C was chosen for the following reasons: although at a temperature of 150 °C the ettringite crystals disintegrate and the decomposition phases of the CAH and CSH gels begin, all this initially has only a minimal effect on the resulting mechanical properties of the concrete [23]. However, this begins to change at a temperature of 500 °C, when the bonds of the final compounds of the CAH gels and $Ca(OH)_2$ begin to break down, causing the formation of CaO together with gaseous CO_2, which, during its expansion and escape from the material, causes the formation of microcracks. This rapid leakage can also cause a high-energy, potentially explosive, breakdown of the surface layer, so-called "chipping" [23,24]. The temperature of 573 °C is considered here to be the limit at which the phase transformation of quartz from a triclinic to a hexagonal system begins, which causes the cohesion between the aggregate and the cement paste to be disrupted due to differences in thermal expansion; here, the volume of the aggregate grains can increase by up to 5% and cause cracks to form, resulting in a large decrease in the strength properties of the material [1,25]. The temperature of 900 °C was chosen mainly because of the temperature milestone of 750 °C, at which the breakdown of the CSH gel bonds begins to peak and the decarbonization of the $CaCO_3$ contained in the aggregate occurs as CO_2 escapes from the compounds. This rapidly released gas, just as in the case of $Ca(OH)_2$ decay, mentioned above, causes great damage to the concrete structure, with the formation of microcracks that continue to reduce the

strength of the concrete [23,24]. At the same time, at such high temperatures, the hydraulic bond in the cement paste changes to a ceramic bond, a process we call concrete sintering, during which the concrete still retains its residual strength. At a temperature of 900 °C, the total decomposition of the cement putty in non-heat-resistant concrete begins [1].

An increasingly topical area in the construction industry is sustainable development, where, in all the phases of the construction life cycle, it is necessary to deal with the economy as well as the impact on the environment. This is most often by trying to reduce the amount of CO_2. The raw material resources themselves also have a limited character, where the construction industry in particular consumes a large portion of them. It is possible to include concrete among the essential building materials. Concrete currently exists in a number of forms. Potentially interesting options include replacing the binder and aggregate with alternative solutions. For example, the possibility of using alkali-activated concrete (AAC), which does not require cement or the replacement of a part of the typical aggregate with a suitable substitute, which includes recycled materials, lightweight aggregates, etc., is very current. There is a wide range of material research where the specialization in a selected area, the properties, or the influence of a specific component of the recipe does not allow for a more comprehensive evaluation and application verification.

For this reason, there is a potential research focus of the structural application of advanced and alternative concrete-based composite systems where alkali-activated concrete (AAC) is chosen as a potentially interesting alternative to the use of lightweight aggregates.

From the point of view of innovation and the scope of the research, it is essential that the proposed parameters of the experimental program do not only include compressive strength but a number of others, including workability and resistance to exposure to elevated temperatures.

The proposed experimental program is designed comprehensively to enable a wider analysis and comparison of the performed tests. For a more complex analysis and comparison, the same raw material base is chosen. The most important parts of the original experimental program are the tests of beams without shear reinforcement, which are supplemented by specialized experiments, which include, for example, pull-off tests. The basic laboratory tests include compressive strength tests, split tensile tests, flexural tensile tests, and modulus of elasticity. The overall designed experimental program will make it possible to present an alternative solution to the simultaneous use of ordinary concrete in reinforced concrete beams without shear reinforcement.

2. Materials

The objective of the experiment is to design concrete mixtures using more eco-friendly and locally available materials. For the purposes of the experiment, 3 mixtures were designed with a mutual characteristic of 450 kg of the main binder component in 1 m^3 of the mixture. The main filler component of all mixtures consisted of a natural crushed aggregate fraction 4/8 from the Litice nad Orlici quarry and a natural mined aggregate fraction 0/4 from the Tovacov gravel and sand pit in Czech Republic. The first reference mixture (REF) used as a binder was Ordinary Portland cement (OPC) CEM I 42.5 R from the Hranice cement plant (Cement Hranice), with the use of a liquid superplasticizer based on polycarboxylate (PC) and polyphosphonate (PS) as admixtures. The local Moravian–Silesian Region retains a considerable amount of heavy steel industry producing large amounts of blast furnace slag, so, in the second mixture, the role of the binder was filled by finely ground granulated blast furnace slag (GGBS) supplied by LB Cemix, s.r.o., Štramberk, Czech Republic, with a specific surface area of 420 kg/m^2 and specific gravity 2850 kg/m^3, in combination with sodium water glass (with silicate modulus *M*s = 2.0 and density of 1500 kg/m^3) and a 50% solution of potassium hydroxide (density of 1500 kg/m^3) to modify the silicate modulus [26]. The plasticizer used was based on modified naphthalene polymers (MNP). This mixture was marked as an alkaline-activated composite (AAC). The third mixture contained the same OPC—CEM I 42.5 R—as the REF mixture, as a binder,

but part of the aggregate used was replaced with keramzit aggregate 1/4 with a density of 500 kg/m^3 so as to lower the density in the lightweight concrete mixture (LC). Keramzit (expanded clay) is a lightweight aggregate composed of a combination of clays that are first granulated and then calcinated (the process whereby, thanks to chemical changes, many pores are created, resulting in a lightweight porous structure), after which they are sintered in rotary kilns at temperatures between 1150 °C and 1250 °C and then gradually cooled to stabilize their final properties. As a result, in addition to its already mentioned lightweight nature, keramzit also has some thermally insulating properties, with good prospects for recyclability and a low impact on natural resources in comparison to natural aggregates derived from mining, mainly thanks to the huge abundance and accessibility of clay. The keramzit was supplied by Liapor Vintířov, Czech Republic. Even though it may not seem like it, the cement to water ratio was also kept similar to that used in the REF mixture w/c = 0.44. In the case of ACC, less straight water was used, but we must keep in mind that the water glass and potassium hydroxide that were used are both aqueous solutions that add more water to the mix. On the other hand, in the LC mixture, more mixing water was used to ensure the sufficient replacement of the water lost via soaking into the porous keramzit aggregate, which should not contribute to the hydration of cement. All mixtures are summarized in Table 1.

Table 1. Mixtures.

Input Materials	(kg/m^3)		
	REF	**AAC**	**LC**
Cement CEM I 42.5 R	450	X	450
Blast furnace slag JMŠ 420		450	
Water glass	X	56.3	X
50% KOH solution		42	
Water	200	172	224
PC and PS based superplasticizer	3	X	3
MNP based plasticizer	X	9	X
0/4 Aggregate	1230	920	1020
4/8 Aggregate	550	670	550
Lightweight keramzit aggregate	X	X	81

3. Results of Experiments

3.1. Preparation of Test Specimens—Testing of Fresh Mixture

During the production of the test samples, the workability tests of the fresh mixes were carried out in accordance with the Czech standards, including flow table tests [27], slump tests [28], and degree of compaction tests [29]. The averaged results are provided in Table 2. The fresh REF and LC mixtures were stiff compared to the very fluid AAC mixture (Figure 1), which, as expected, also achieved significantly faster solidification than the fresh REF and LC mixtures.

Table 2. Fresh mixture workability test results.

	REF	**AAC**	**LC**
Flow table test (mm)	290	660	260
Slump test (mm)	20	250	30
Degree of compaction (-)	1.13	1.02	1.13



(**a**) (**b**) (**c**)

Figure 1. Results of slump test: (**a**) REF, (**b**) AAC, and (**c**) LC.

3.2. Bulk Density

The bulk density was determined from the average values of all the tested samples. The values of the REF and AAC are very similar to each other, as can be seen in Figure 2. In the case of the comparison with the LC, where part of the aggregate included in the previous mixtures was replaced with an artificial lightweight aggregate, the average bulk density was more than 100 kg/m^3 lower, which equates to a more than 5% difference in bulk weight.

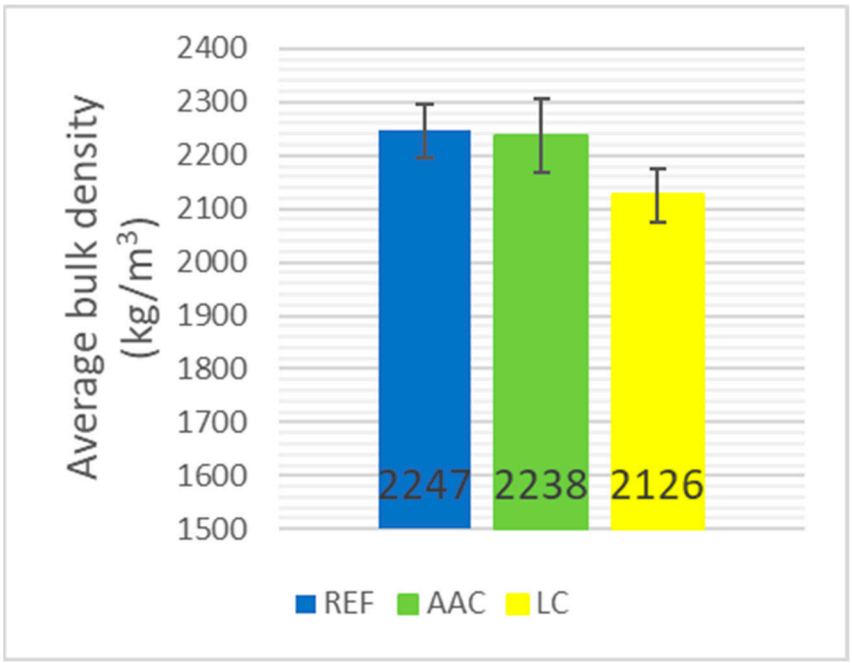

Figure 2. Average bulk density results.

3.3. Strength Characteristics

All the strength characteristics were also tested in accordance with the Czech standards. Two sample shapes were chosen for testing. The compressive strength [30] and split tensile strength [31] were tested on cube-shaped samples with an edge length of 150 mm. The second variant used consisted of prisms with a size of 40 × 40 × 160 mm, on which both the compressive strength [32] and prism flexural strength [32] were tested. Diagrams of the test procedures can be seen in Figure 3.

The cubic compressive strength of the REF was, on average, 12.4 MPa lower than that of the AAC, and, comparing the REF with the LC, on the contrary, the average strength was found to be higher, by 9.2 MPa. In the case of the prism's compressive strength, the difference between the individual mixtures was lower. When the REF was compared to the AAC, the highest compressive strengths were measured for the AAC, which were 23%

higher for the cubic bodies and 12.5% higher for the prisms compared to the REF. In the case of the comparison of the REF and LC, the difference was similarly determined to be 16.5%, regardless of the sizes and shapes of the tested samples. A graphical comparison can be seen in Figure 4.

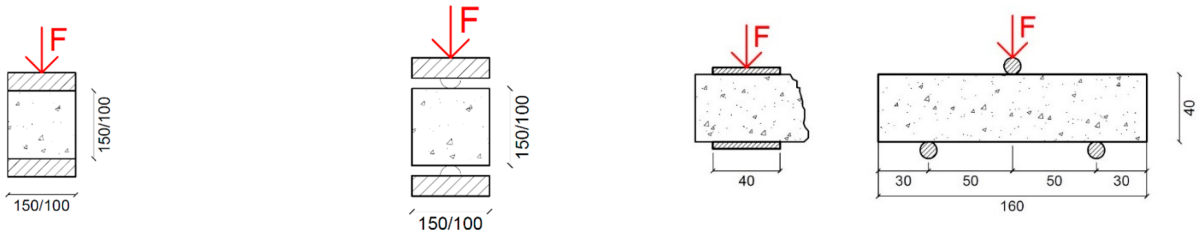

(**a**) (**b**) (**c**)

Figure 3. Diagrams of (**a**) compressive strength test, (**b**) split tensile strength test, and (**c**) prism compressive and flexural strength tests.

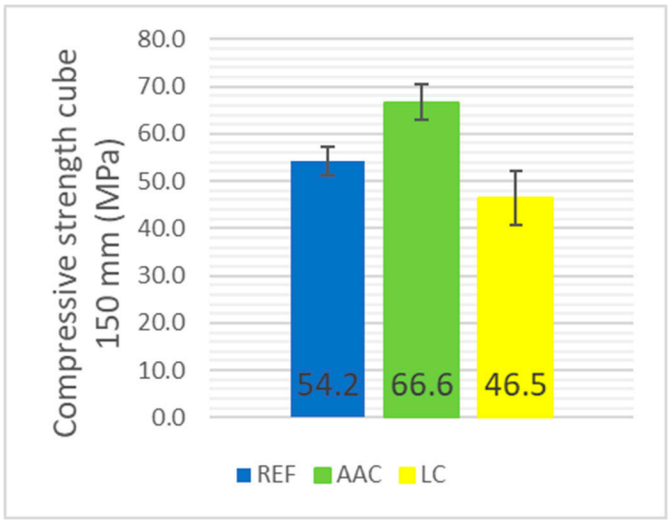

(**a**)

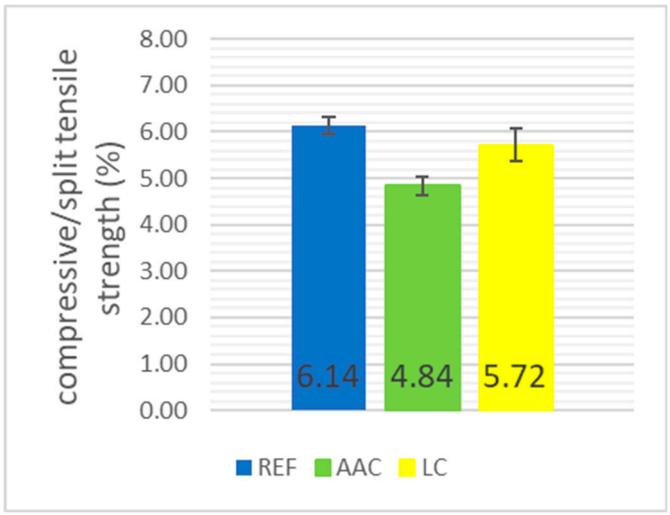

(**b**)

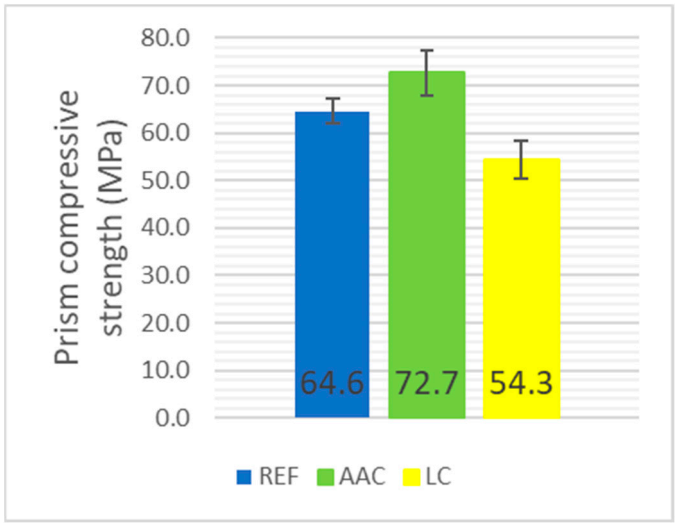

(**c**)

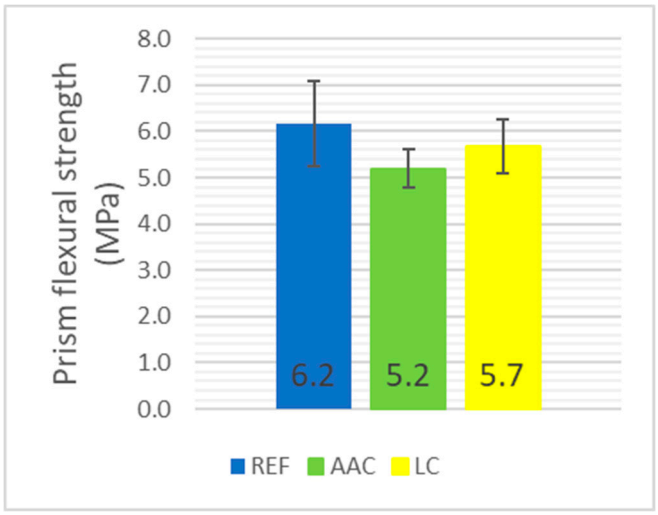

(**d**)

Figure 4. Strength characteristics of tested mixtures: (**a**) compressive strength, (**b**) compressive/split tensile strength ratio, (**c**) prism compressive strength, and (**d**) prism flexural strength.

Figure 5 shows the tested prisms, where the characteristic features of each of the mixtures used are visible in the cross-section; the LC differs from the REF by the presence of "black particles" of porous keramzit grains, while the AAC is characterized by a greenish color caused by the presence of sulfides in the hydration products.



(**a**) (**b**) (**c**)

Figure 5. Inner structure of tested samples: (**a**) REF, (**b**) AAC, and (**c**) LC.

3.4. Static Modulus of Elasticity

There are several methods available for determining the static modulus of elasticity; in this case, the ČSN EN 12390-13 B standard [33] was used, in which the basic and upper stress are maintained for 20 s. Figure 6 shows typical load (a) and deformation (b) curves measured for one of the REF mixture samples.

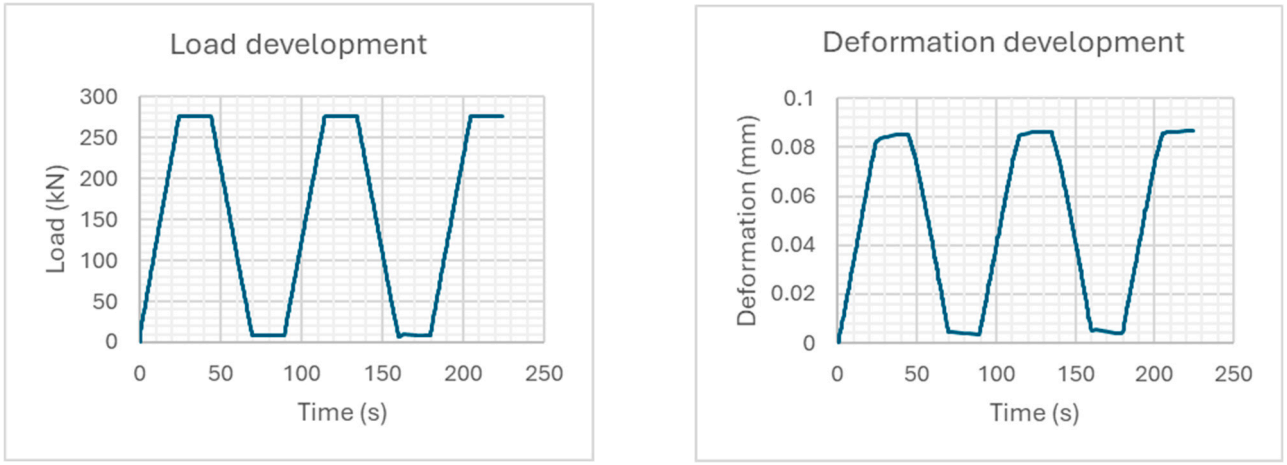

(**a**) (**b**)

Figure 6. Typical (**a**) load development and (**b**) deformation development for REF mixture.

The highest values were achieved by the cement-based mixtures. The REF reached 28.2 GPa, while the LC showed 7.8% lower and the AAC showed 17% lower average values than the REF (Figure 7b). In Figure 7a, one can see the REF sample equipped with sensors for testing the static modulus of elasticity at 1/4 and 3/4 of the body height.

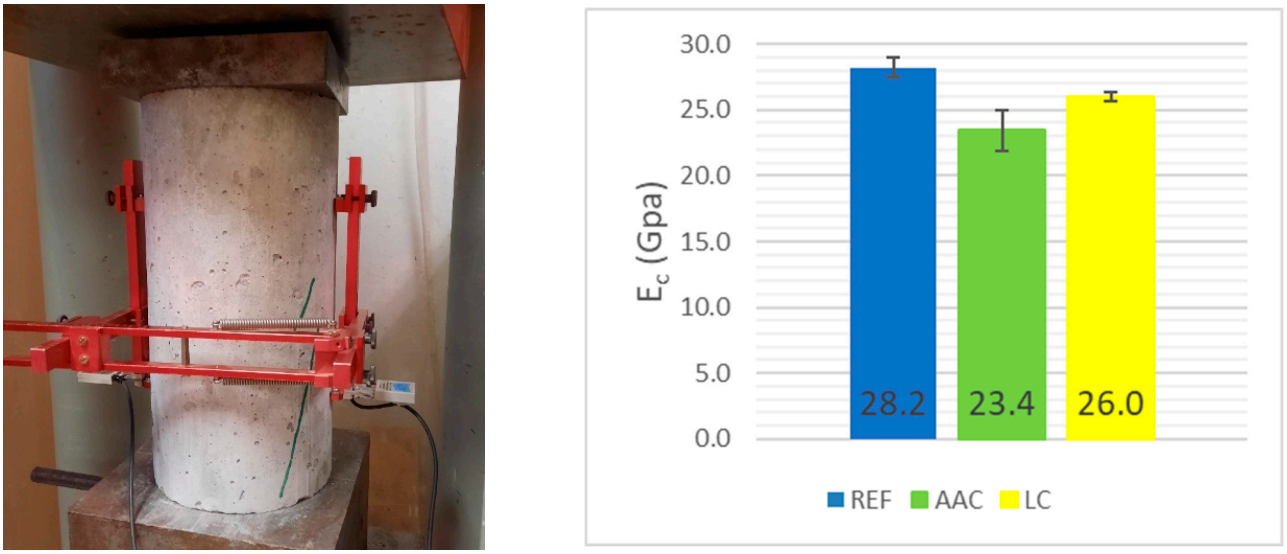

(**a**) (**b**)

Figure 7. (**a**) Sample set for testing of static modulus of elasticity; (**b**) static modulus of elasticity results.

3.5. Heat Resistance

The purpose of the test was to simulate the heat load, for which a laboratory chamber furnace LAC K120/12 was used. As testing samples, we again used prism-shaped samples with dimensions of 40 × 40 × 160 mm on which the speed of passage of the ultrasonic pulse (Figure 8) was tested to determine the degree of damage to the microstructure of the material [34]. Subsequently, tensile bending and compression tests were also performed.

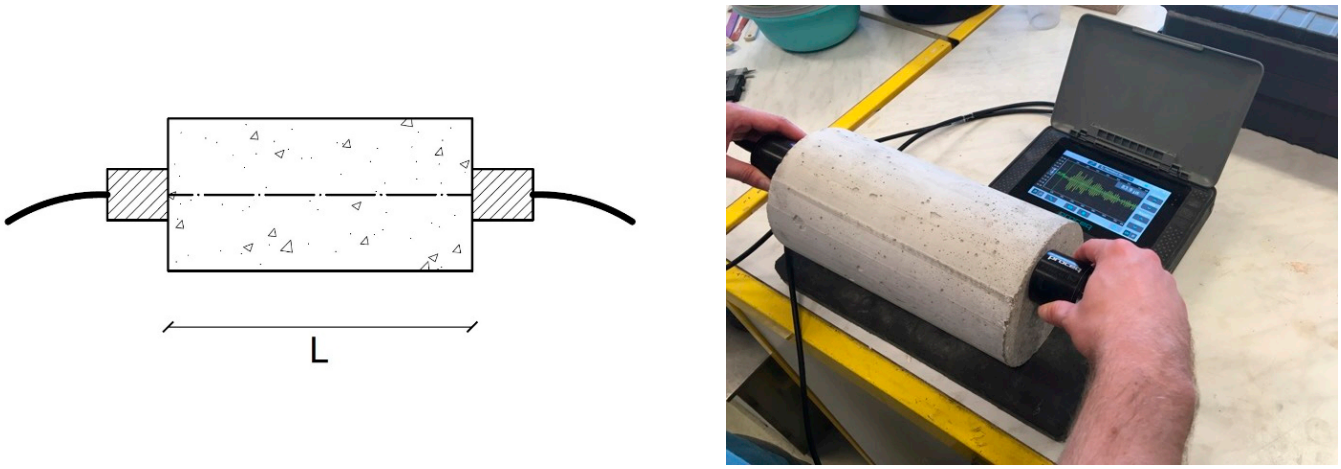

(**a**) (**b**)

Figure 8. Ultrasonic pulse testing method: (**a**) diagram; (**b**) testing on cylindric sample.

The temperatures chosen for comparison were 20, 105, 600, and 900 °C. The temperature of 20 °C simulates the behavior at normal temperatures, and the results were demonstrated in Section 3.3. The samples tested at temperatures of 600 and 900 °C were dried at a temperature of 105 °C before exposure to heat for safety reasons so as to avoid the explosive separation of the surface layer and thus damage to the test equipment during the rapid increase to high temperatures. During this drying, the free and physically bound water in the pores and capillaries will evaporate, at which point the positive effect of a slight increase in strength can be expected. For this reason, this temperature was also included in the experiment. After drying, the test samples were put in a laboratory furnace, wherein the temperature was increasing at a rate of 200 °C per hour until a set temperature

was achieved. The target temperature was maintained for 2 h, after which the furnace doors were opened to cause "rapid" cooling.

As mentioned above, before comparing the resulting properties after exposure to heat, before the destructive measurement of the compressive strength and bending flexural strength, the degree of damage to the internal microstructure of the tested materials was also determined using the ultrasonic pulse method, during which the speed of the passage of the ultrasonic wave was measured. As can be seen in Figure 9, there was no change when it was exposed to air temperature and dried at 105 °C in the case of the OPC. However, when testing the samples after exposure to 600 °C, the velocity of the UZ wave decreased by about 65% in the case of the materials with OPC and by 75% in the case of the AAC. When tested after exposure to 900 °C, both the REF and LC again dropped by approximately 78% compared to the initial measurement; in the case of the AAC, the values could no longer be determined using the given method. It is, therefore, assumed that alkaline-activated composites based on GGBS are more susceptible to internal failure due to high temperatures compared to OPC.

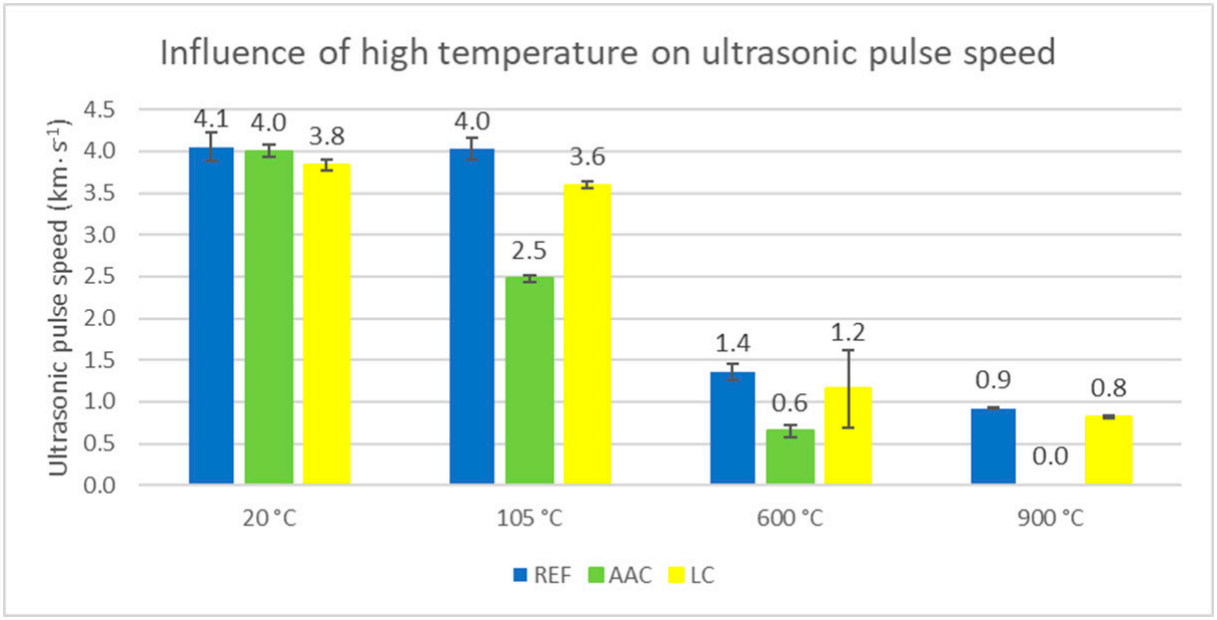

Figure 9. Effect of temperature on ultrasonic pulse test.

When comparing the strength characteristics, after drying at 105 °C, we see a slight increase in the compressive strength and a significant increase in the flexural bending strength of the OPC mixtures REF and LC. However, with the AAC, after drying, there was a slight decrease in both measured strength characteristics, as a result of which it can be concluded that the removal of water from pores and capillaries can have a positive effect on cement mixtures, while applying the alternative binder GGBS in combination with activators can have negative effects. At the next measured temperature point of 600 °C, a drastic decrease in the measured values of both tested strength characteristics was already noticeable, when, just as under normal conditions, the AAC reached higher compressive strength values (Figure 10) and lower values in bending tension (Figure 11) than both recipes containing OPC. After exposure to a temperature of 900 °C, the strengths found were very low. Although the bodies still held their shape, they disintegrated (crumbled) with the slightest application of force.

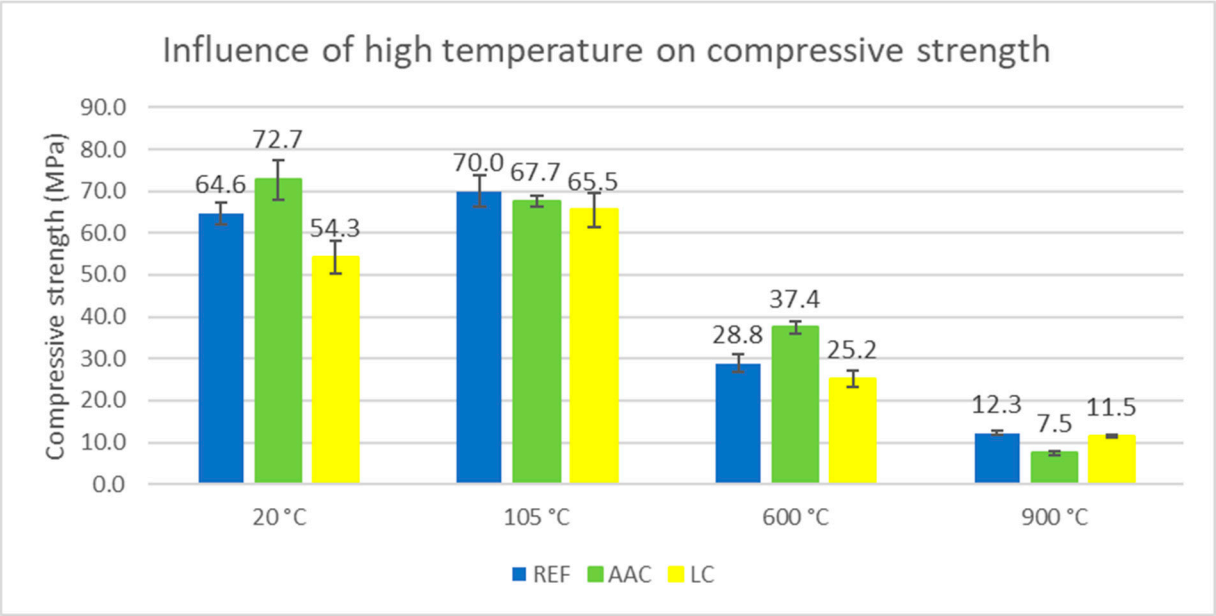

Figure 10. Effect of temperature on compressive strength.

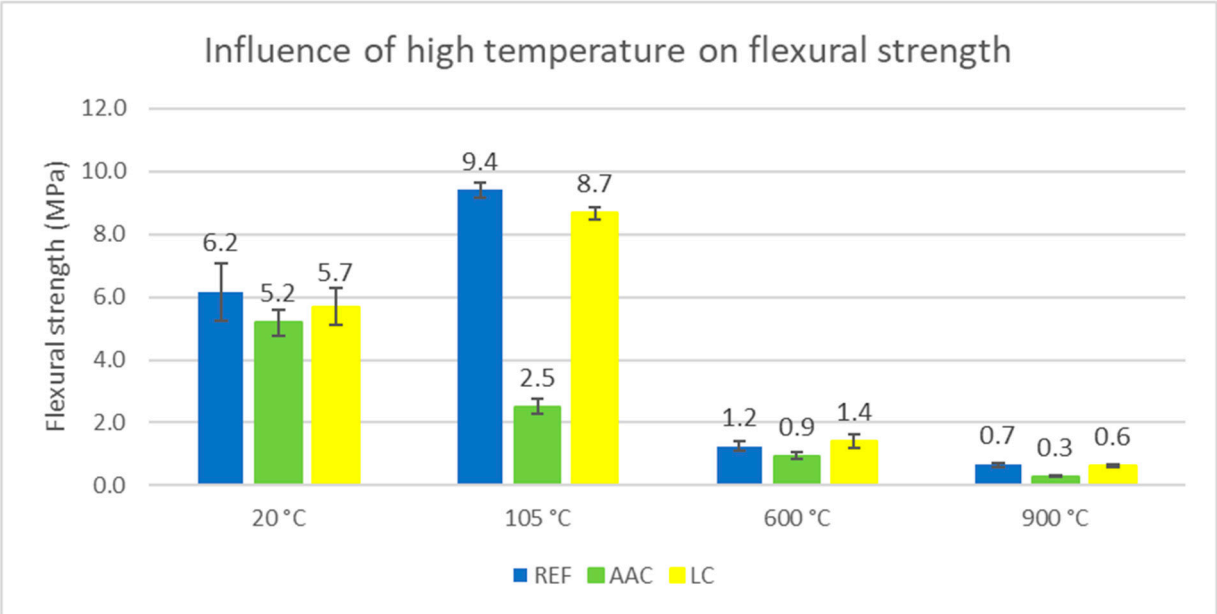

Figure 11. Effect of temperature on flexural strength.

Apart from influencing the mechanical properties of the tested samples, there was also a visible change in color due to the temperature. For the OPC-based mixtures REF (Figure 12a) and LC (Figure 12b), a transition from gray to a pinkish color could be seen at 600 °C, which then returned to gray but of a lighter shade at 900 °C. In the case of the AAC mixture (Figure 12c), the color changed from light beige to orange at 600 °C and to pink at 900 °C.

The observation of the microstructures of both types of concrete was carried out using an SEM at a magnification of 1000 times. Figure 13 shows the REF mixture's microstructure before and after exposure to 600 °C. The samples were applied to double-sided carbon tape attached to the aluminum target holder and sputtered with an approximately 30 nm-thick Pt layer using a Quorum Q150V ES plus (Quorum Technologies Ltd., Lewes, UK) device. The samples were studied using a scanning electron microscope (SEM) JEOL JSM-7610F

Plus (JEOL, Tokyo, Japan) in BSE mode (accelerating voltage 30 keV) with secondary electron detection.

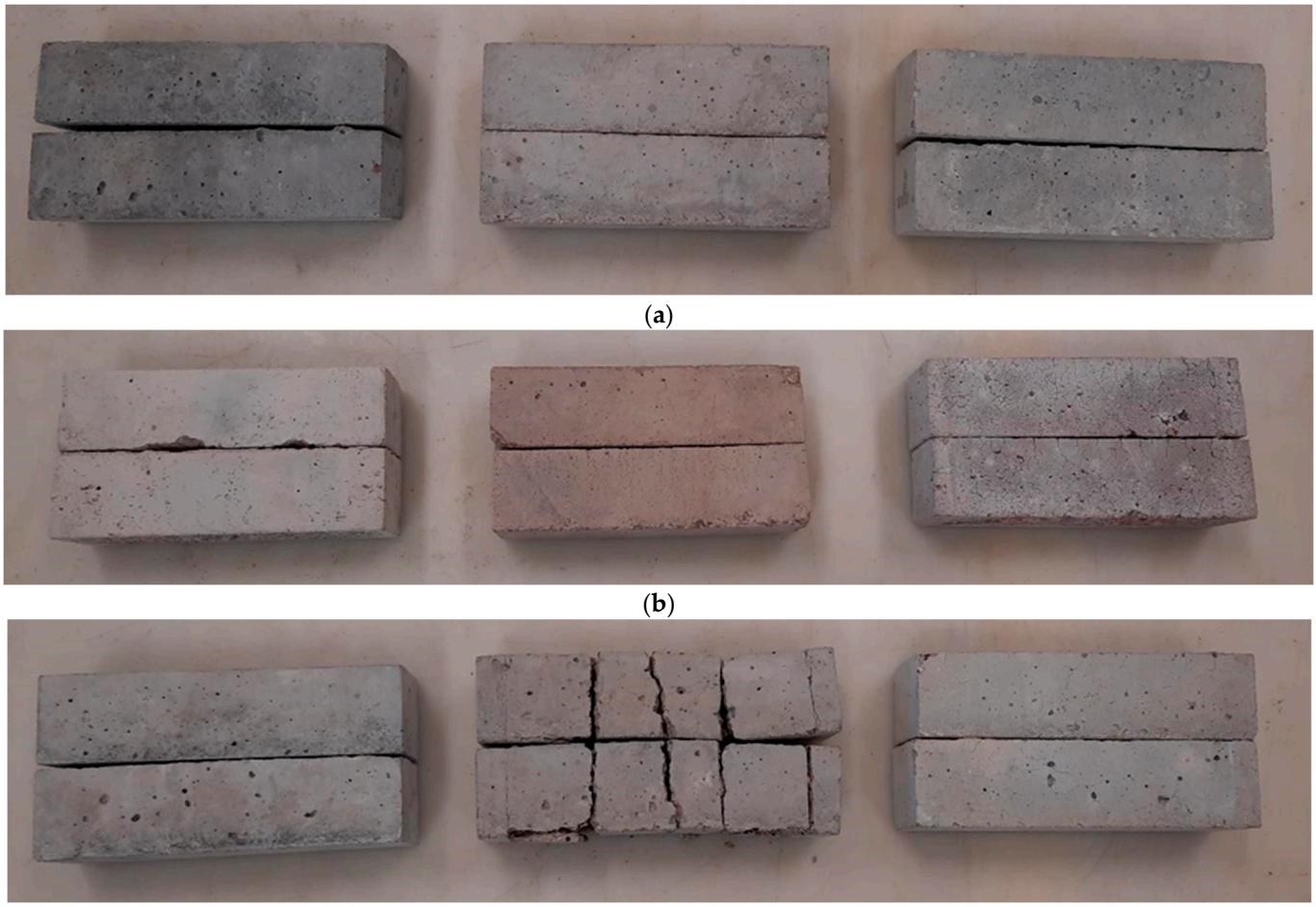

(**a**)

(**b**)

(**c**)

Figure 12. Color change of the test samples for (from the left) 20 °C, 600 °C, and 900 °C: (**a**) REF, (**b**) AAC, and (**c**) LC.

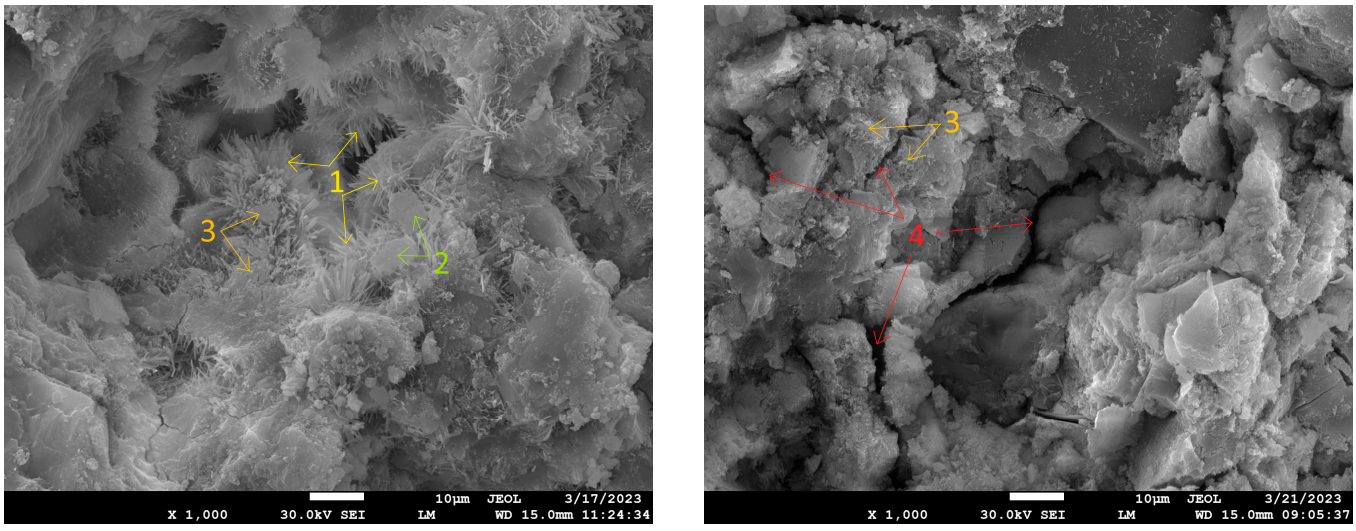

(**a**) (**b**)

Figure 13. Pictures of REF mixture taken using an electron microscope: (**a**) 20 °C; (**b**) 600 °C.

Figure 13a clearly shows the presence of needle-like crystals of ettringite (1), plate-like crystals of Portlandite $Ca(OH)_2$ (2), and CSH gel (3). On the contrary, in Figure 13b after exposure to 600 °C, the absence of ettringite and Portlandite is noticeable, while, on the other hand, we can still see the CSH gel (3). The most noticeable change was the creation of a large amount of microcracks (4) created either by the phase transformation of quartz or the release of gaseous CO_2 from decaying Portlandite compounds.

3.6. Load Capacity of Reinforced Concrete Beams

As can be seen from the diagram in Figure 14, to test the load capacity, reinforced concrete beams with a length of 1150 mm and a cross-section of 100 × 190 mm were manufactured, and the span during the loading test was 900 mm. The dimensions of the beams were selected with reference to the previous research conducted by our colleagues [4,20].

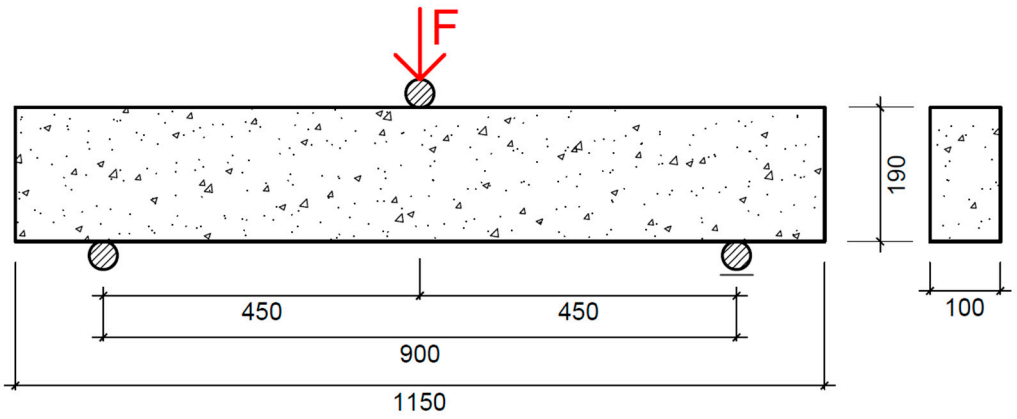

Figure 14. Diagram of the load capacity test of the reinforced concrete beams used.

The evaluation of the overall load capacity of the reinforced concrete beams and the designation of the beams are shown in Table 3. This table also shows an evaluation of the experiments of bearing capacity in comparison with the calculated values, where, in all the cases, the load capacity reached in the experiments was greater than that provided by the theoretical calculation model. It is a common feature of all load diagrams that the bending stiffness of the beams depends more significantly on the degree of longitudinal reinforcement than on the concrete mix used. The total maximum bearing capacity also depends more significantly on the degree of reinforcement. Overall, the maximum load ranges from 40.7 kN to 65.4 kN.

Table 3. Load capacity of reinforced concrete beams depending on reinforcement and mixture.

Number of Reinforcements Ø 10 mm	Load Capacity (kN)				V_{exp}/V_R (-)		
	REF	AAC	LC	LC (First Peak)	REF	AAC	LC
1	40.7	43.2	41.9	41.9	1.28	1.26	1.31
2	45.5	52.5	55.7	49.1	1.13	1.21	1.39
3	58.9	65.4	57.9	50.0	1.28	1.32	1.26

When using 1 × Ø 10 mm reinforcement, the load diagrams (Figure 15) are very similar for all three concrete mixtures. Tensile cracks produced by bending are typical for these beams (Figure 16). The first cracks appeared directly under the load at the lower edge, and, gradually, other cracks appeared closer to the supports. As the load gradually increased, the cracks opened, and the concrete near the load was also damaged. The maximum deformation ranged from approximately 12.5 mm for the REF beam to 24 mm for the LC beam and 17 mm for the beam with the AAC mixture, which also reached the highest load capacity of 43.2 kN.

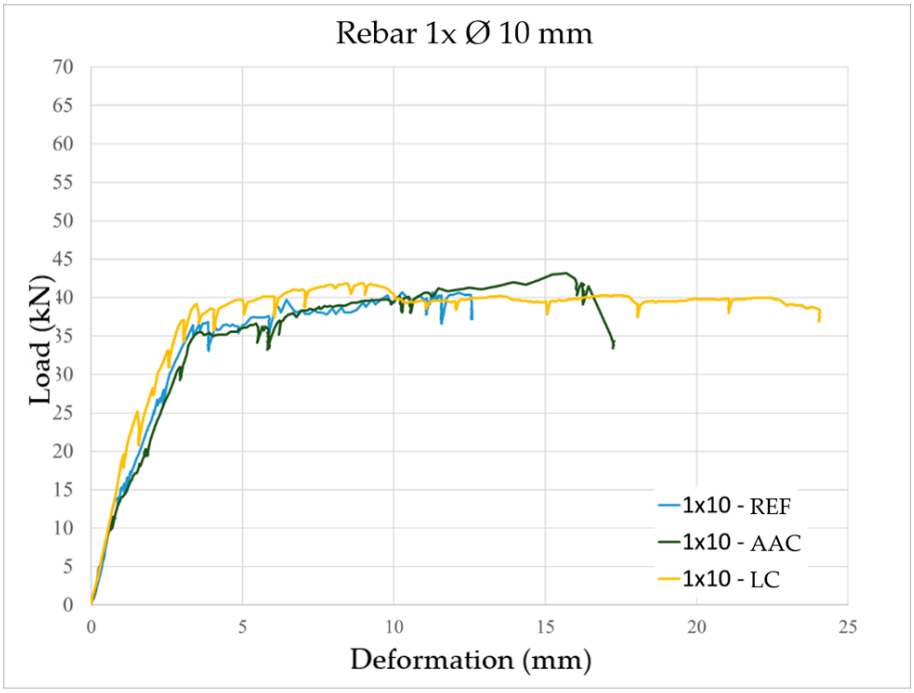

Figure 15. Load diagram of reinforced concrete beams—1 × Ø 10 mm.



Figure 16. Pictures of tested reinforced concrete beams with 1 × Ø 10 mm rebar: (**a**) REF, (**b**) AAC, and (**c**) LC, (number indicates initiation crack formation process).

In the case of another reinforcement variant with two concrete reinforcements—2 × Ø 10 mm—the results are not so clear-cut. The maximum load was reached by the LC concrete mixture, but it should be noted that the load diagram (Figure 17) includes a significant load drop. The drop in the load was also accompanied by the development of a shear crack in the concrete. In all the cases, the beam collapse mechanism was characterized by a

form of shear crack (Figure 18). The bearing capacity of the beam composed of the AAC with 52.5 kN was again greater than that of the reinforced concrete beam composed of the ordinary concrete REF, which reached 45.5 kN. Surprisingly, even the beam composed of the lightweight concrete LC had a higher load capacity of 49.1 kN; i.e., the maximum load capacity achieved was 55.7 kN. In the load diagram for the LC, a significant jump can be seen, which was influenced by the development of a new shear crack. The maximum deformations for the beams composed of the LC and REF ranged around 4 mm, while that for the beam composed of the AAC reached 8 mm.

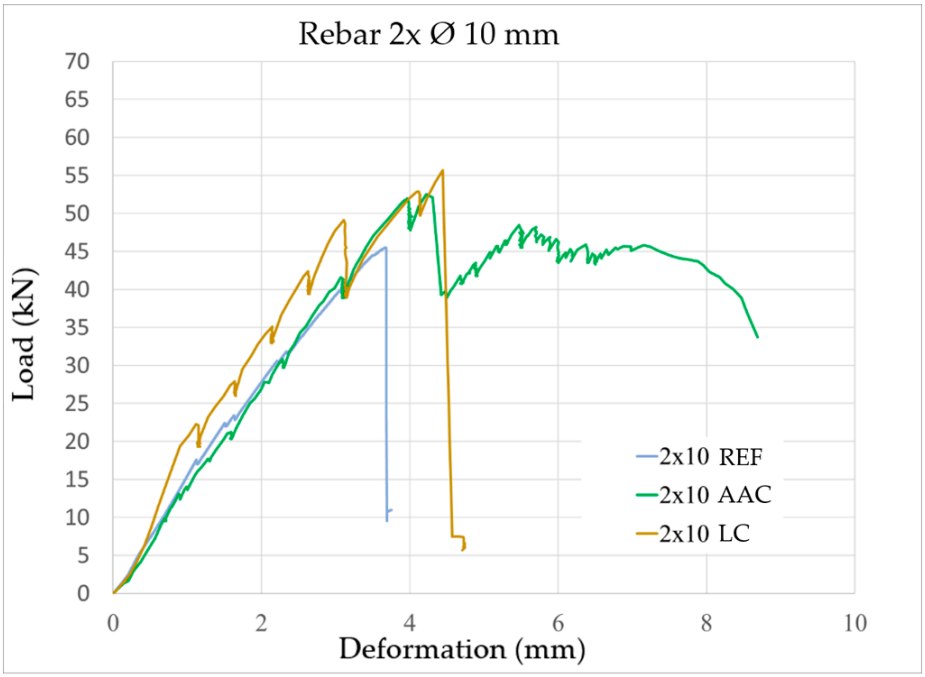

Figure 17. Load diagram of reinforced concrete beams—2 × Ø 10 mm.

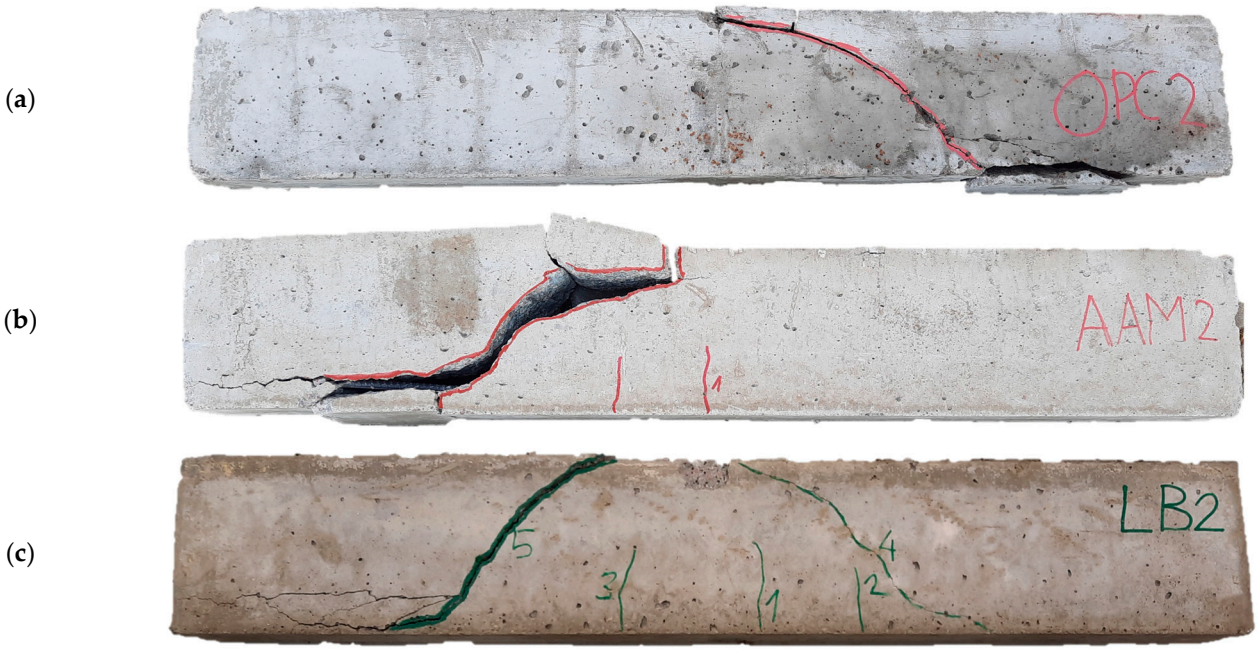

Figure 18. Pictures of tested reinforced concrete beams with 2 × Ø 10 mm rebar: (**a**) REF, (**b**) AAC, and (**c**) LC, (number indicates initiation crack formation process).

In the third variant of the reinforced concrete beams with three concrete reinforcements Ø 10 mm, the highest load capacity was again found in the variant composed of an AAC mixture with 65.4 kN. In second place was the beam composed of the REF mixture, reaching 58.9 kN. The lowest load capacity was reached by the reinforced concrete beam created from a concrete LC mixture with 50.0 kN and 57.9 kN, respectively. Again, in the case of the LC beam, the loading diagram (Figure 19) shows two phases of loading during the initiation and development of shear cracks. The first load decrease was most probably caused by the loosening of one of the rebars from the rest of the material, after which the loading continued until the beam failed. In the case of the third beam variant, the mechanism was typically significantly more fragile, with little ductility. In all the cases, the reason for the collapse was a typical shear crack (Figure 20). The longitudinal reinforcement also significantly affected the amount of deformation of the third variant, which amounted to 3–4 mm at the maximum load. Considering that, in all the cases, the collapse of the beams was caused by concrete failure, there was no rupture in the concrete reinforcement.

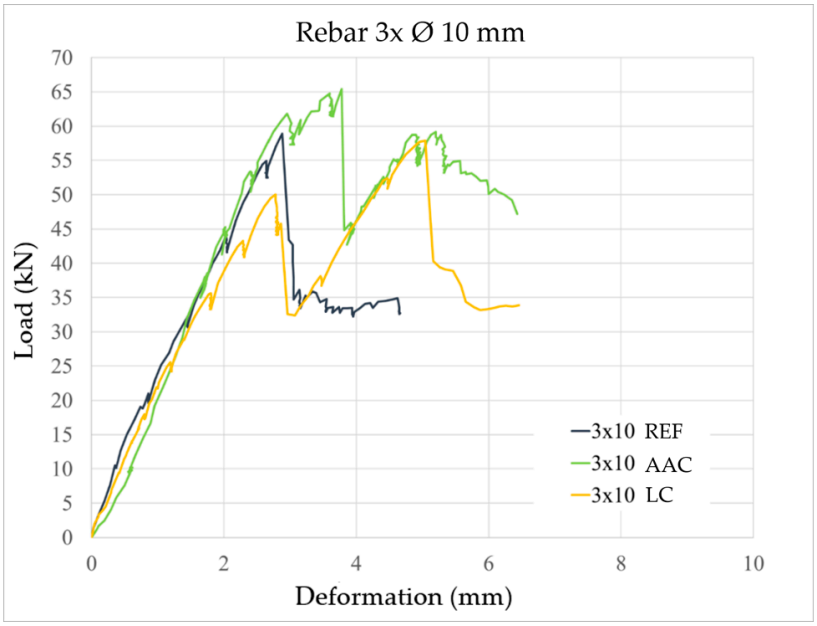

Figure 19. Load diagram of reinforced concrete beams—3 × Ø 10 mm.

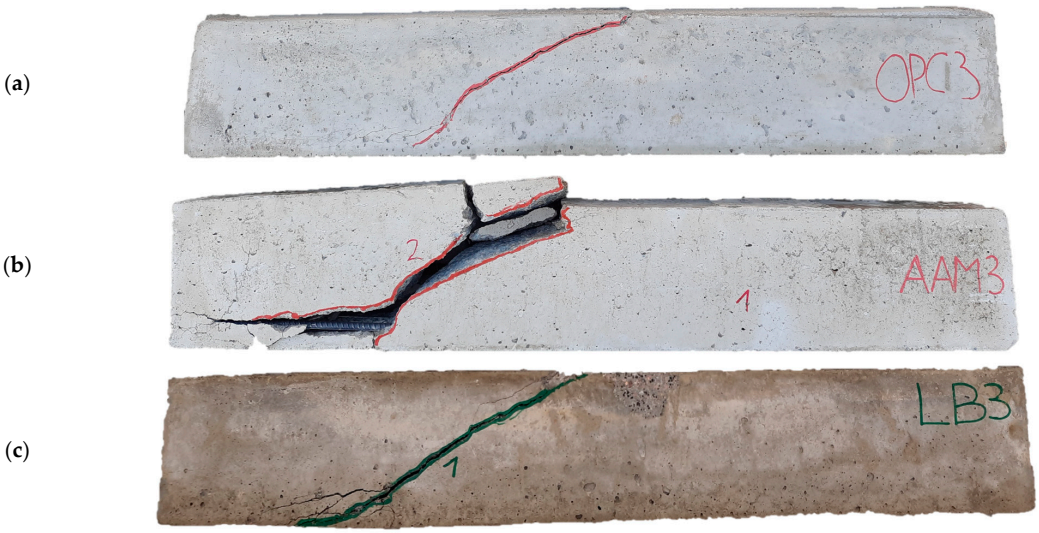

Figure 20. Pictures of tested reinforced concrete beams with 3 × Ø 10 mm rebar: (**a**) REF, (**b**) AAC, and (**c**) LC, (number indicates initiation crack formation process).

3.7. Tensile Strength of Surface Layer

The tests applied to the reinforced concrete beams without shear reinforcement also assessed the tensile strength of the surface layers after the completion of static load tests. The final test results are shown in Figure 21. In the case of the beams composed of the REF and LC cement mixtures, the values of the tensile strength of the surface layer were very similar. The average values were 3.66 MPa for the beams composed of the OPC concrete and 3.75 for the lightweight concrete, but, in both cases, there was a large dispersion in the measured values, with a standard deviation of 0.83 MPa for the REF and 0.96 MPa for the LC. The tensile strengths of the beams created from the AAC mixture were significantly lower than the measured strengths of the REF and LC, by approximately half. The average measured strength was 1.64 MPa, but the dispersion of the values obtained by the measurement was also lower when the standard deviation was about 0.18 MPa. Figure 22 shows a test being carried out on a sample.

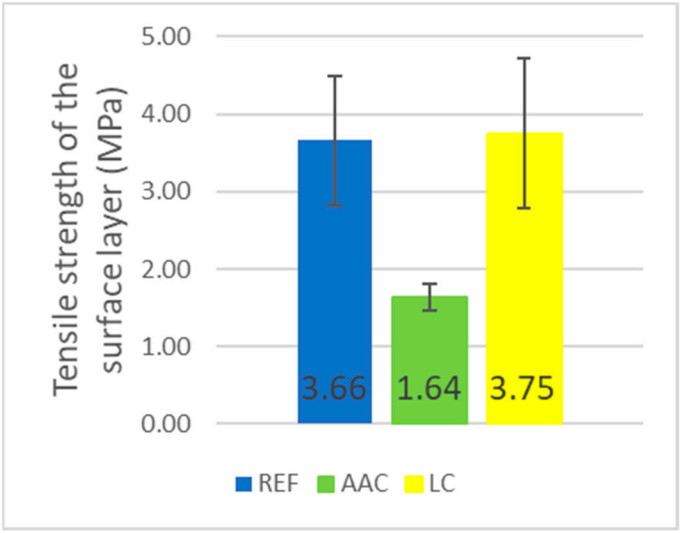

Figure 21. Results regarding the tensile strengths of the surface layers.

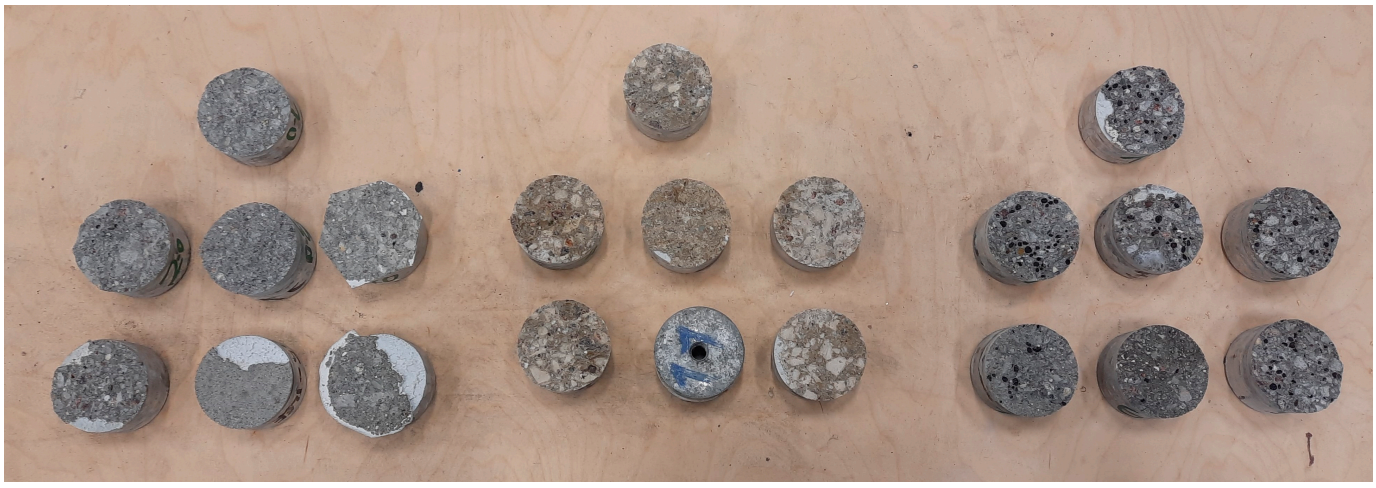

Figure 22. Showcase of the tensile strengths of surface layer test samples.

4. Discussion

The broader goal of the research and experiments [35,36] is the structural application of advanced and alternative concrete-based composite systems, where, in view of the research to date, it is possible to use, for example, alkaline-activated concrete (AAC) as a potentially interesting alternative, or to use lightweight aggregates. It is essential

from the point of view of the design application that the design parameters do not only include compressive strength but a number of others, including workability and durability. However, material research often focuses only on a selected property, typically compressive strength, without further details on other properties. However, the proposed experimental program is designed more comprehensively and enables a wider analysis and comparison of the performed tests. For a more complex analysis and comparison, the same raw material base was chosen. The highest compressive strengths were obtained for the AAC when it was an alternative cement-free binder system solution. However, it is important to note that the static modulus found for this material was the smallest and the compressive and transverse tensile strength ratios were also lower. The stated results and ratio can be considered expected with regard to the previous research. Among the basic properties of the AAC mixture is that a large amount of spillage was achieved in the fresh mixes test. The lowest total compressive strengths were recorded for LC. The mentioned variant of concrete included the lightened expanded keramzit aggregate. As expected, there was a reduction in the bulk density. Specifically, the LC density was 2130 kg/m^3, which is more than 100 kg/m^3 less than the other two mixes. A side effect of the use of the lightweight aggregates was the burning of the mechanical properties when there was a decrease in strength (16.5%). At the same time, there was also a deterioration in other material properties, but, overall, it is possible to assess that the decline was not fundamental. The elastic modulus values of the tested mixtures ranged from 23.4 to 28.2 GPa, with both the LC and AAC mixtures showing lower elastic modulus values compared to the conventional concrete using OPC. A previous study [37] was concerned with determining the mechanical properties of alternative cement-free materials, such as geo-polymer concrete. In experimental programs involving GGBS [38–41], the resulting elastic moduli were very similar to those observed in our study, but our composite showed greater compressive strength. Compared to another experimental program [42], the compressive strength values collected by us were again similar, but the elastic modulus was significantly lower.

In the experimental program, we also noted technological differences during the production of the mixtures, which were verified by performing selected tests on the fresh mixtures. In terms of the cement mixtures, there were no problems with the processing time. However, despite its high fluidity, the cement-free AAC mixture solidified very quickly and lost its workability, as is typical for alkali-activated materials.

The essential results of the experimental program also include the evaluation of resistance to high temperatures, which is closely related to the structural design, where fire resistance is also a very important design criterion. Based on the above, temperatures of up to 900 °C were chosen as part of the experimental program. Considering temperatures of 20 °C, 600 °C, and 900 °C, there was a decreasing trend in the measured properties with rising temperature. In the case of 105 °C, whereat the residual water in concrete is evaporated, the ultrasonic speed and flexural strength test results decreased significantly in the case of the AAC (by more than 1/3) in comparison to 20 °C; on the other hand, the flexural strength of the OPC-based mixtures was increased by 1/3 of its former values. This may imply that GGBS-based binders are more vulnerable to the lower spectrum of high temperatures.

The core part of this study consisted of experiments on reinforced concrete beams without shear reinforcement. In total, nine experiments were performed on three beams with different degrees of reinforcement in each mixture. The experiments confirmed that the degree of longitudinal reinforcement has the most significant influence on the overall load-bearing capacity. In individual series of beams with the same degree of reinforcement, the failure mechanisms were very similar. The specific bearing capacity values differed, but the differences were not fundamental. The maximum load capacity was achieved with the AAC. The key and very significant results can be considered the technological success in the production of beams from the AAC, where the static tests verified the design possibilities, the mechanism of damage, and the collapse of the structure itself. The above is essential and provides the possibility to use AAC not only on a laboratory scale but also for

building elements. In the conducted experiments, the emergence of typical tensile cracks from bending and shear cracks was monitored with regard to the degree of reinforcement of the beam. The interaction of the reinforcement with the concrete was also verified, such as with the AAC.

The tensile strengths of the surface layer, assessed by the pull-off test, were very similar for both the REF and LC mixtures, but both also showed similarly high variances in their results, with no dependence on the specific surface or beam tested. The AAC mixture's surface layer strength was less than half that of its OPC counterparts. This could have been caused by the high shrinkage, which is caused by the chemical composition of GGBS. This surface layer vulnerability was also confirmed during the testing of frost resistance and resistance against defrosting chemicals, which is not part of this paper.

5. Conclusions

The main goal of this article was to present a comprehensive experimental program [35] that included three different mixtures. To compare the results of the experimental program, the mixtures were designed regarding the raw materials. Small aggregates of the 4–8 mm fraction from the Litice granite and the sand fraction of 0–4 mm were taken from the Tovacov gravel and sand pit. Portland cement (CEM I 42.5 R) was used as the first reference mixture (REF). The initial dosage was set at 450 kg of cement. In the second mixture, the cement used as a binder was replaced with an alternative. Specifically, this was an alkaline-activated composite (AAC), where 450 kg of finely ground granulated blast furnace slag (GGBS), sodium water glass, and potassium hydroxide were used. The third mixture was a modified version of the first, wherein part of the aggregate was replaced with lightweight aggregate keramzit (LC). The experimental program included tests of compressive strength, split tensile strength, flexural strength, and the static modulus of elasticity. These tests were followed by another specialized test to determine the effect of high temperatures, up to 900 °C.

Regarding its mechanical parameters, the AAC mixture overall showed similar or slightly better results, except in terms of the flexural strength and static modulus of elasticity. Also, its resistance against high temperatures seemed very similar, except at the 105 °C measurement point, which is not particularly beneficial.

All three variants represented an alternative material solution for the construction of beams without shear reinforcement. The failure mechanisms for all the cases of longitudinal reinforcement showed similar characteristics to the reinforced concrete beams without shear reinforcement, composed of a typical OPC (REF). The possible applications of alkaline-activated materials are mainly technological as it is appropriate to use them in the prefabrication of structural elements. In the case of technological solutions with longer workability, a wider range of possible applications are also offered by the elements concreted on site. For AAC applications, it is necessary to pay increased attention to the verification of the design parameters. The residual strengths of the AAC show a similar decreasing trend with respect to increasing temperature. The tensile strengths of the surface layer were similar for both OPC mixtures but were halved in the case of the AAC. However, the AAC shows significantly lower CO_2 production. Using keramzit as the artificial aggregate is also a relatively eco-friendly approach, mainly in comparison to natural aggregate mining. However, substituting in the chosen amount of this material may not seem worth it considering that it only offers a slight decrease in the bulk density with a proportionally greater loss in the mechanical properties.

Among the key conclusions and benefits of the experimental program is that it was possible to produce beams from the AAC mixture, which is a technological success. Static tests verified the mechanism of damage and collapse of the beams themselves. This result is crucial because it enables the use of AAC not only in laboratory conditions but also for building elements. For beam experiments, the typical tensile cracks caused by bending and shear cracks will appear during the tests, depending on the degree of reinforcement of the beam and loading.

Author Contributions: Conceptualization, O.S.; methodology, V.B.; validation, J.J.; formal analysis, J.J.; investigation, J.J.; resources, J.J.; data curation, R.G. (Radoslav Gandel), R.G. (Roman Gabor) and J.J.; writing—original draft preparation, J.J. and Z.M.; visualization, Z.M.; supervision, V.B.; project administration, O.S. All authors have read and agreed to the published version of the manuscript.

Funding: This research was funded by the Jan Amos Komensky Operational Program financed by the European Union, grant number CZ.02.01.01/00/22_008/0004631 Materials and technologies for sustainable development.

Institutional Review Board Statement: Not applicable.

Informed Consent Statement: Not applicable.

Data Availability Statement: The data presented in this study are available at Zenodo https://doi.org/10.5281/zenodo.11191475 (accessed on 14 May 2024).

Acknowledgments: This research was conducted with financial support from the Ministry of Education, specifically the Student Research Grant Competition of the Technical University of Ostrava under identification number SP2024/072. This paper was also created as part of project No. CZ.02.01.01/00/22_008/0004631 Materials and technologies for sustainable development within the Jan Amos Komensky Operational Program financed by the European Union and the state budget of the Czech Republic.

Conflicts of Interest: The authors declare no conflicts of interest.

References

1. Collepardi, M. *The New Concrete*; ENCO: Ponzano, Italy, 2006; p. 420. ISBN 88-961469-4-X.
2. Aïtcin, P.C. *High-Performance Concrete*, 1st ed.; CRC Press: London, UK, 1998; p. 624. ISBN 9780429204074.
3. Mateckova, P.; Bilek, V.; Sucharda, O. Comparative Study of High-Performance Concrete Characteristics and Loading Test of Pretensioned Experimental Beams. *Crystals* **2021**, *11*, 427. [CrossRef]
4. Sucharda, O.; Marcalikova, Z.; Gandel, R. Microstructure, Shrinkage, and Mechanical Properties of Concrete with Fibers and Experiments of Reinforced Concrete Beams without Shear Reinforcement. *Materials* **2022**, *15*, 5707. [CrossRef] [PubMed]
5. Fischetti, M.; Bockelman, N. Concrete Cure. Online. *Sci. Am.* **2023**, *328*, 52. [CrossRef]
6. Hájek, P. Principles of sustainability in designing concrete structures according to MC2020. In Proceedings of the Conference 28. Concrete Days, ČBS, Praha, Czech Republic, 19–20 May 2022. (In Czech).
7. Palomo, A.; Monteiro, P.; Martauz, P.; Bilek, V.; Fernandez-Jimenez, A. Hybrid binders: A journey from the past to a sustainable future (*opus Caementicium futurum*). *Cem. Concr. Res.* **2019**, *124*, 105829. [CrossRef]
8. García-Lodeiro, I.; Palomo, A.; Fernández-Jiménez, A. Hybrid alkaline cements: Hydration kinetics study during the early reaction stages. In Proceedings of the 5th International Conference on Non-Traditional Cement & Concrete, Brno, Czech Republic, 16–19 June 2014; pp. 59–62, ISBN 978-80-214-4867-4.
9. Özkılıç, Y.O.; Zeybek, Ö.; Bahrami, A.; Çelik, A.İ.; Mydin, M.A.O.; Karalar, M.; Hakeem, I.Y.; Roy, K.; Jagadesh, P. Optimum usage of waste marble powder to reduce use of cement toward eco-friendly concrete. *J. Mater. Res. Technol.* **2023**, *25*, 4799–4819. [CrossRef]
10. Bilek, V.; Sucharda, O.; Bujdos, D. Frost Resistance of Alkali-Activated Concrete—An Important Pillar of Their Sustainability. *Sustainability* **2021**, *13*, 473. [CrossRef]
11. Kothari, A.; Habermehl-Cwirzen, K.; Hedlund, H.; Cwirzen, A. A Review of the Mechanical Properties and Durability of Ecological Concretes in a Cold Climate in Comparison to Standard Ordinary Portland Cement-Based Concrete. *Materials* **2020**, *13*, 3467. [CrossRef]
12. Lee, J.; Lee, T.; Lee, S.; Choi, H. Performance Evaluation of Cementless Composites with Alkali-Sulfate Activator for Field Application. *Materials* **2020**, *13*, 5410. [CrossRef] [PubMed]
13. Collins, F.; Sanjayan, J.G. Workability and mechanical properties of alkali activated slag concrete. *Cem. Concr. Res.* **1999**, *29*, 455–458. [CrossRef]
14. Awoyera, P.; Adesina, A. A critical review on application of alkali activated slag as a sustainable composite binder. *Case Stud. Constr. Mater.* **2019**, *11*, e00268. [CrossRef]
15. *ČSN EN 1992-1-1*; Eurocode 2: Design of Concrete Structures—Part 1-1: General Rules and Rules for Building Structures, 2nd ed. Office for Technical Standardization, Metrology and State Testing: Prague, Czech Republic, 2019.
16. Classen, M. Shear Crack Propagation Theory (SCPT)—The mechanical solution to the riddle of shear in RC members without shear reinforcement. *Eng. Struct.* **2020**, *210*, 110207. [CrossRef]
17. Mari, A.; Cladera, A.; Bairan, J.M.; Oller, E.; Ribas, C. Shear-flexural strength mechanical model for the design and assessment of reinforced concrete beams subjected to point or distributed loads. *Front. Struct. Civ. Eng.* **2014**, *8*, 337–353. [CrossRef]
18. Fernandez Ruiz, M.; Muttonia, A.; Sagasetab, J. Shear strength of concrete members without transverse reinforcement: A mechanical approach to consistently account for size and strain effects. *Eng. Struct.* **2015**, *99*, 360–372. [CrossRef]

19. Muttoni, A.; Fernandez Ruiz, M. From experimental evidence to mechanical modeling and design expressions: The Critical Shear Crack Theory for shear design. *Struct. Concr.* **2019**, *20*, 1464–1480. [CrossRef]
20. Sucharda, O. Identification of Fracture Mechanic Properties of Concrete and Analysis of Shear Capacity of Reinforced Concrete Beams without Transverse Reinforcement. *Materials* **2020**, *13*, 2788. [CrossRef] [PubMed]
21. Marcalikova, Z.; Cajka, R.; Bilek, V.; Bujdos, D.; Sucharda, O. Determination of Mechanical Characteristics for Fiber-Reinforced Concrete with Straight and Hooked Fibers. *Crystals* **2020**, *10*, 545. [CrossRef]
22. Özkılıç, Y.O.; Althaqafi, E.; Bahrami, A.; Aksoylu, C.; Karalar, M.; Özdöner, N.; Shcherban, E.; Stel'makh, S.; Beskopylny, A.; Thomas, B.S.; et al. Influence of ceramic waste powder on shear performance of environmentally friendly reinforced concrete beams. *Sci. Rep.* **2024**, *14*, 10401. [CrossRef] [PubMed]
23. Collier, N.C. Transition and Decomposition Temperatures of Cement Phases—A Collection of Thermal Analysis Data. *Ceram. Silik.* **2016**, *60*, 338–343. [CrossRef]
24. Kučera, P.; Češelská, T.; Matečková, P. *Fire resistance of Building Structures*; SPBI: Ostrava, Czech Republic, 2010; ISBN 978-80-7385-094-4. (In Czech)
25. Pospíšil, D. Mineralogical Composition of Dinas. Bachelor's Thesis, University of Technology, Brno, Czech Republic, 2018.
26. Szklorzová, H.; Bilek, V. Influence of alkali ions in the activator on the performance of alkali activated mortars. In Proceedings of the 3rd International Symposium Non-Traditional Cement and Concrete, Brno, Czech Republic, 10–12 June 2008; pp. 777–784.
27. *ČSN EN 12350-5*; Testing Fresh Concrete—Part 5 Flow Table Test. The Czech Office for Standards, Metrology and Testing: Prague, Czech Republic, 2020.
28. *ČSN EN 12350-2*; Testing Fresh Concrete—Part 2 Slump Test. The Czech Office for Standards, Metrology and Testing: Prague, Czech Republic, 2020.
29. *ČSN EN 12350-4*; Testing Fresh Concrete—Part 4 Degree of Compatibility. The Czech Office for Standards, Metrology and Testing: Prague, Czech Republic, 2020.
30. *ČSN EN 12390-3*; Testing Hardened Concrete—Part 3: Compressive Strength of Test Specimens. The Czech Office for Standards, Metrology and Testing: Prague, Czech Republic, 2020.
31. *ČSN EN 12390-6*; Testing Hardened Concrete—Part 6: Tensile Splitting Strength of Test Specimens. The Czech Office for Standards, Metrology and Testing: Prague, Czech Republic, 2024.
32. *ČSN EN 196-1*; Methods of Testing Cement—Part 1: Determination of Strength. The Czech Office for Standards, Metrology and Testing: Prague, Czech Republic, 2016.
33. *ČSN EN 12390-13*; Testing Hardened Concrete—Part 13: Determination of Secant Modulus of Elasticity in Compression. The Czech Office for Standards, Metrology and Testing: Prague, Czech Republic, 2021.
34. *ČSN 73 1371*; Non-Destructive Testing of Concrete—Method of Ultrasonic Pulse Testing of Concrete. The Czech Office for Standards, Metrology and Testing: Prague, Czech Republic, 2011.
35. Dataset Zenodo. Available online: https://zenodo.org/records/11191475 (accessed on 14 May 2024).
36. Jerabek, J. Reinforced Concrete Beams without Shear Reinforcement. Master's Thesis, VSB-TU Ostrava, Ostrava, Czech Republic, 2022.
37. Mohammed, A.A.; Ahmed, H.U.; Mosavi, A. Survey of Mechanical Properties of Geopolymer Concrete: A Comprehensive Review and Data Analysis. *Materials* **2021**, *14*, 4690. [CrossRef]
38. Yang, K.-H.; Cho, A.-R.; Song, J.-K. Effect of water–binder ratio on the mechanical properties of calcium hydroxide-based alkali-activated slag concrete. *Constr. Build. Mater.* **2012**, *29*, 504–511. [CrossRef]
39. Venu, M.; Rao, T.D.G. An experimental investigation of the stress-strain behavior of geopolymer concrete. *Slovak J. Civ. Eng.* **2018**, *26*, 30–34. [CrossRef]
40. Raut, U.; Shalini, A.; Prabu, B. Strength of geopolymer concrete reinforced with basalt fiber. *Int. Res. J. Eng. Technol.* **2019**, *6*, 3811–3817.
41. Nath, P.; Sarker, P.K. Flexural strength and elastic modulus of ambient-cured blended low-calcium fly ash geopolymer concrete. *Constr. Build. Mater.* **2017**, *130*, 21–31. [CrossRef]
42. Sarvanan, S.; Elavenil, S. Strength properties of geopolymer concrete using M-sand by assessing their mechanical characteristics. *ARPN J. Eng. Appl. Sci.* **2018**, *13*, 4028–4041.

Disclaimer/Publisher's Note: The statements, opinions and data contained in all publications are solely those of the individual author(s) and contributor(s) and not of MDPI and/or the editor(s). MDPI and/or the editor(s) disclaim responsibility for any injury to people or property resulting from any ideas, methods, instructions or products referred to in the content.